Pressure-Induced Melting and Crystallization of Poly(ethylene oxide)

Weisheng Li and Maciej Radosz*

Exxon Research and Engineering Company, Annandale, New Jersey 08801

Received February 12, 1992; Revised Manuscript Received May 11, 1992

ABSTRACT: A new 2-kbar optical cell is developed for cloud-point measurements on polymer films. Pressure dependence of melting points and crystallization temperatures for poly(ethylene oxide) (PEO), measured in this cell, is found to be linear up to 200 MPa (2000 bar). Slopes (dT_m/dP) of 0.111, 0.126, and 0.126 °C/MPa are obtained independently from optically measured cloud points, from P–V–T data, and from estimates based on the Clapeyron equation using DSC data, respectively. Our approximation of the Clapeyron equation, which requires only the apparent ambient-pressure properties of a semicrystalline polymer, is demonstrated to be consistent with the high-pressure experimental data. Also, P–V–T properties obtained for PEO melts are correlated with three equations of state.

Introduction

In general, pressure induces molecular order and, hence, shifts polymer melting (T_m) and crystallization (T_{crys}) transitions to higher temperatures. It is important to understand the pressure dependence of T_m and T_{crys} from both practical (material structure–property relationships) and theoretical (free volume, compressibility effects) viewpoints. There are four high-pressure experimental techniques used for studying polymer phase transitions: dilatometry, cloud point, microscopy, and calorimetry. Zoller and co-workers[1–8] developed a high-pressure dilatometer (P–V–T apparatus) and studied a number of crystalline polymers (Nylon-66, PEEK, PET, poly(4-methylpentene-1), PTFE, and poly(oxymethylene)) using this apparatus. Gogolewski and Pennings[9–12] observed crystallization and melting of a series of nylons in a piston cell up to 10 kbar. Hiramatsu and co-workers[13] reported a high-pressure optical cell with sapphire windows for studying morphologies and kinetics of PET and PE crystallization. Also high-pressure DTA was used for studies on polymer blend phase separation[14] and polymer glass transitions.[15]

In addition to the experimental approaches, one can also estimate the pressure dependence of the melting and crystallization temperatures from the Clapeyron equation.[16] For example, for melting, the Clapeyron equation can be written as follows:

$$\frac{dT_m}{dP} = T_m\frac{\Delta V_m}{\Delta H_m} \tag{1}$$

where ΔV_m and ΔH_m are the volume change and enthalpy change upon melting, respectively. Zoller and co-workers[1–8] used this equation to estimate the heat of fusion for pure polymeric crystals.

By contrast, one of the objectives of this work is to use the apparent values of ΔV_m, ΔH_m, and T_m of *semicrystalline* poly(ethylene oxide) obtained from ambient-pressure measurements to estimate the pressure dependence of T_m. Other objectives are to determine dT_m/dP from cloud-point and P–V–T experiments and to correlate the P–V–T properties of PEO melts with equations of state.

Experimental Section

High-Pressure Optical Cell. PEO phase transitions are measured at high pressures in an optical cell shown in Figure 1.

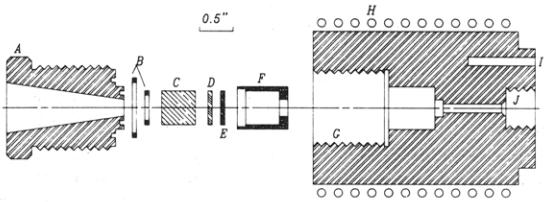

Figure 1. High-pressure optical cell for measuring cloud points: (A) SS gland, (B) Viton O-rings, (C) sapphire window, (D) sample film, (E) metal foil, (F) brass cap, (G) cell body, (H) electric heater, (I) thermocouple well, (J) pressurizing fluid port.

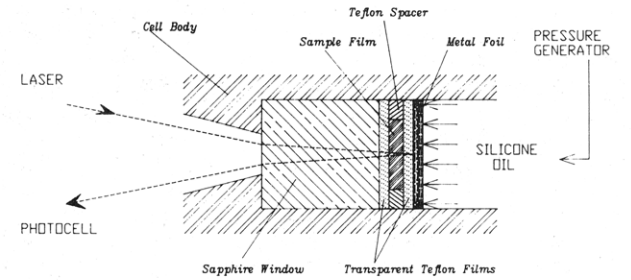

Figure 2. Principle of the reflect-mode cloud-point measurements at high pressures. Polymer film is exposed to uniform pressure but not to the pressurizing fluid.

The main parts of the cell are a stainless steel body (G), a gland (A), and a sapphire window (C, 0.500 × 0.500 in.). A flexible heater (H) and a layer of insulation (not shown in Figure 1) allow for temperature control. This cell is demonstrated to work up to 200 MPa at 300 °C. The sample film is placed between the sapphire window and a metallic mirror. The mirror is made of a flexible aluminum foil coated on polyester film provided by ICI Films (MELINEX Advance 451/200 gauge). The whole window set (window, sample, and mirror) is attached to the gland with a brass cap (F) and pressurized by silicone oil (Dow Corning, No. 210H).

A more detailed view of the window set is shown in Figure 2. In order to prevent the silicone oil from getting in contact with the polymer, the sample film is sandwiched between two transparent Teflon sheets and surrounded by a Teflon spacer (Du Pont Electronics, Catalog Nos. A200 and A500, respectively). A laser beam passing through the sample film is reflected by the mirror to a photodetector. The intensity of the reflected beam is plotted against temperature (linear increase). During a melting transition, upon heating, the reflected beam intensity increases dramatically due to the increased sample clarity. Conversely, during crystallization, upon cooling, the reflected beam intensity decreases due to the increased sample turbidity (cloudiness).

The overall experimental setup is illustrated in Figure 3. A computerized syringe pump, filled with silicone oil, controls the cell pressure. A temperature programmer (Valley Forge Instru-

* To whom correspondence should be addressed.

0024-9297/93/2226-1417$04.00/0

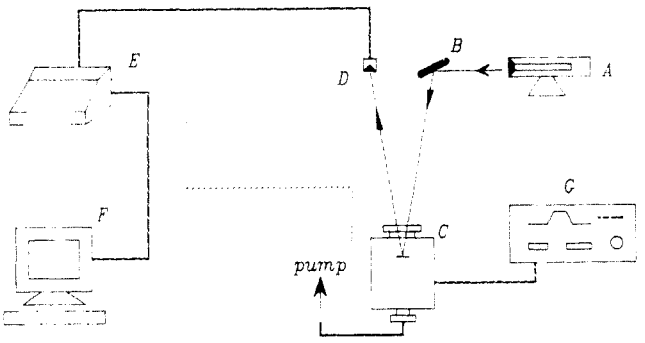

Figure 3. Schematic view of the reflect-mode cloud-point apparatus: (A) HeNe laser, (B) mirror, (C) high-pressure cell, (D) photodetector, (E) Mettler FP80HT processor, (F) IBM PC, (G) temperature programmer.

ment Company, Model PC6040S) controls the cell temperature. A Mettler FP80HT microprocessor receives the temperature and light intensity signals and forwards them to an IBM personal computer. A HeNe laser tube (Uniphase U-1508, 0.5 mW, λ = 632 nm) serves as the light source.

***P–V–T* Apparatus.** Pressure–volume–temperature measurements (*P–V–T*) are carried out using a dilatometer-type[8,17] *P–V–T* apparatus (Gnomix, Inc.). This instrument, which requires a 1.0-cm^3 sample, allows for two kinds of experiments: isothermal compression and isobaric thermal expansion. The *isothermal compression* temperature range is 30–130 °C, and the pressure range is 0–200 MPa; PEO specific volumes are automatically determined every 10 MPa at 4 °C intervals. In *isobaric thermal expansion* experiments, the sample is heated at a constant pressure from 30 to 130 °C, and then it is cooled down to 30 °C. Specific volume changes are measured every 1 °C. Subsequently, the sample is compressed to another pressure and undergoes another heating and cooling cycle. The heating and cooling rates are +1 and −1 °C/min, respectively.

Differential Scanning Calorimeter. DSC measurements are conducted on a Seiko DSC220C differential scanning calorimeter. The sample size is 19 mg. The experimental procedure is as follows: (1) scan the sample from 30 to 120 °C at a rate of 5 °C/min, (2) then cool it back to 30 °C at a rate of −1 °C/min, and (3) reheat the sample from 30 to 120 °C at 1 °C/min. The purpose for the first step is to erase the sample thermal history. Therefore, only results from the second and third steps are recorded. These results are the temperature and heat of melting and crystallization, T_m and ΔH_m, and T_{crys} and ΔH_{crys}, respectively.

Materials. Poly(ethylene oxide) (PEO), purchased from Scientific Polymer Products Inc. (Catalog No. 136A), has average molecular weights of $\bar{M}_w$ = 78 900 and $\bar{M}_n$ = 33 500 as determined by GPC. The PEO powder is initially dissolved in dimethylformamide (DMF). A 0.005-in.-thick film, cast from the DMF solution, is annealed under vacuum at 70 °C to remove the residual solvent. Since the polymer crystallinity depends on its thermal history, all measurements (cloud-point, *P–V–T*, and DSC) are conducted on a sample having the same thermal history (from the melt state, 1.0 °C/min cooling down to 25 °C).

Results and Discussion

PEO Melting from Cloud-Point Data. Semicrystalline polymers contain two domains, crystalline and amorphous, which have different densities. Since the high-density domains scatter light, the semicrystalline polymers become cloudy at temperatures below their melting points and become transparent upon melting. In addition to the difference between the amorphous and crystalline density, light scattering depends on birefringence and the presence of crystalline units that are large enough to interact with light.

A typical cloud-point trace recorded from the high-pressure optical cell is illustrated in Figure 4. We plot the intensity of the reflected main beam versus temperature for PEO at 80 MPa (heating rate of 1.0 °C/min). The

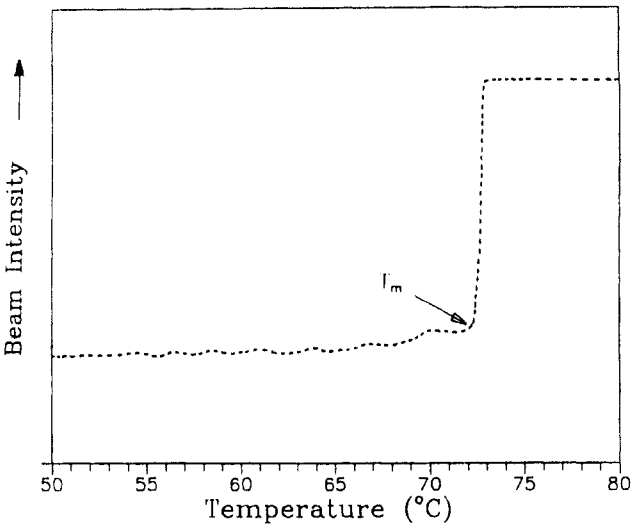

Figure 4. Cloud-point trace for PEO at 80 MPa.

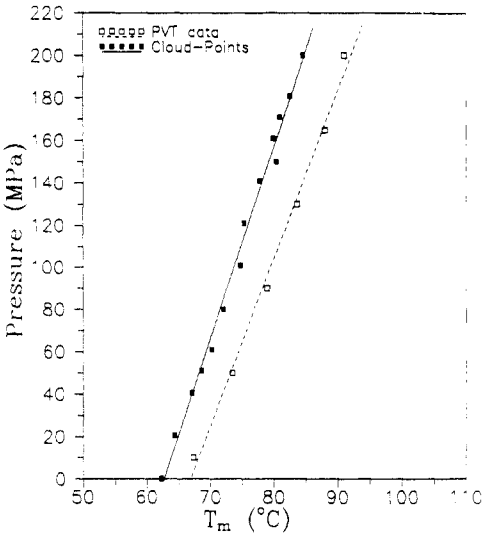

Figure 5. Pressure dependence of PEO melting points obtained from cloud-point and *P–V–T* measurements, respectively.

clear, abrupt increase in the detected beam intensity represents the melting transition and corresponds to T_m.

A plot of pressure versus the optically measured T_m is shown in Figure 5 with filled squares. A linearly regressed slope (dT_m/dP) is found to be essentially constant in the pressure range of 0–200 MPa, equal to 0.111 °C/MPa. Also, for comparison, Figure 5 shows PEO melting points derived from *P–V–T* experiments (open squares) which are described below.

PEO Melting and Crystallization from *P–V–T* Data. A typical *P–V–T* result obtained from an isobaric thermal expansion experiment is shown in Figure 6 where specific volumes are plotted versus temperature at 130 MPa. The isobar shown in Figure 6 allows for determination of T_m and ΔV_m (the melting expansion). Although Starkweather et al.[7] use the end transition point as T_m, we define T_m as the middle point of the melting transition. This is because T_m should correspond to a peak on the differential *P–V–T* isobar (as in DSC and DTA traces), which falls roughly in the middle of the melting transition range on the original *P–V–T* isobar. Also, the middle point is found to be less dependent on the heating rate than the upper end of the melting transition. The T_m and ΔV_m data determined here are summarized in Table I.

A series of similar isobars at different pressures, from 10 to 200 MPa, are shown in Figure 7. As in the cloud-point experiments, increasing pressures not only reduce

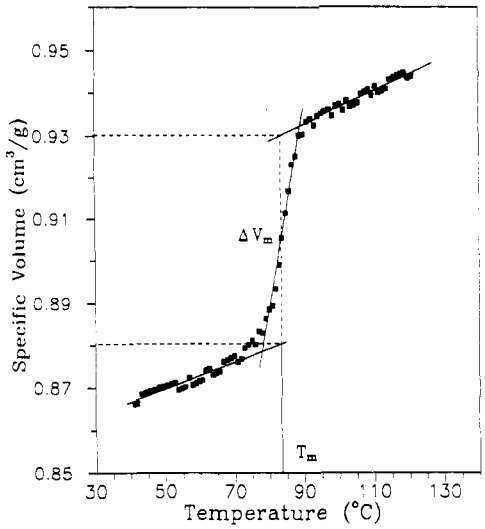

Figure 6. Determination of T_m and ΔV_m^{semi} from isobaric measurements (an example at 130 MPa).

Table I
Summary of *P–V–T* Data for PEO

P (MPa)	ΔV_m (cm³/g) heating	ΔV_m (cm³/g) cooling	T_m (°C) heating	T_m (°C) cooling	$(\partial V/\partial T)_p$ (10^4 cm³/K·g) heating	$(\partial V/\partial T)_p$ (10^4 cm³/K·g) cooling
0	0.0616[a]	0.0615[a]	66.9[a]	47.9[a]		
10	0.063	0.061	67.3	50.0	6.510	6.596
50	0.056	0.056	73.5	54.1	5.595	5.719
90	0.051	0.051	79.0	59.5	3.842	4.932
130	0.048	0.045	83.6	63.0	3.852	4.361
165	0.047	0.044	88.0	67.6	3.376	4.031
200	0.044	0.039	91.0	74.6	3.443	3.957

[a] Extrapolated data.

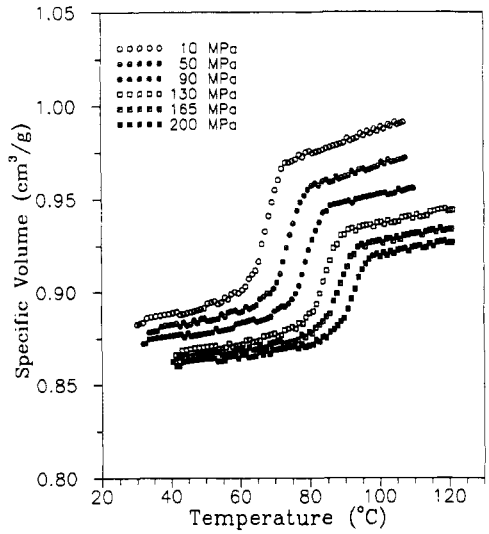

Figure 7. *P–V–T* data: specific volumes of poly(ethylene oxide) as a function of temperatures, obtained at constant pressures (isobaric heating).

specific volume but also shift the melting point to higher temperatures, as shown in Figure 5. The T_m pressure dependence, dT_m/dP, is found to be 0.126 °C/MPa for the data shown in Figures 5 and 7. This is close to dT_m/dP of 0.111 °C/MPa found in the cloud-point experiments, considering that these results are obtained from different methods relying on completely different properties (optical vs volumetric).

However, *P–V–T* results obtained from isothermal compression experiments (rapid compression from 0.1 to 200 MPa at constant temperatures) are quantitatively different in that the melting point difference due to

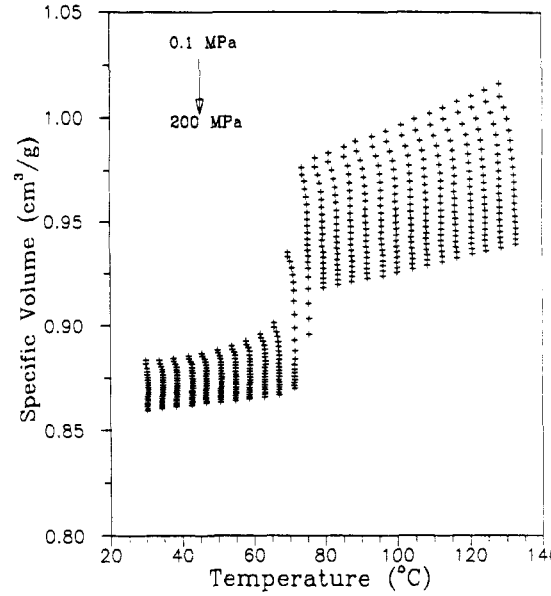

Figure 8. *P–V–T* data: specific volumes of poly(ethylene oxide) obtained at constant temperatures (isothermal compression experiments).

Table II
DSC Data for PEO

run no.	peak temp (T_m or T_{crys}, °C)	ΔH_m (ΔH_{crys}) (J/g)	heating rate (°C/min)
1	70.1	195.5	5
2	47.8	(−162.9)	−1
3	64.4	164.8	1

pressure is much smaller. For example, the difference in melting point between 0.1 and 200 MPa is only about 5 °C. This is illustrated in Figure 8 and can be explained by the fact that in the isothermal compression experiments there is not enough time for the polymer to crystallize (at each higher pressure after the low-pressure melting). In other words, kinetically limited crystallization prevents us from getting accurate melting point measurements. Therefore, we will only use the isobaric thermal expansion data for further analysis.

In addition to the kinetically induced differences between isothermal compression and isobaric expansion, we observe kinetically induced differences between melting and crystallization in the isobaric experiments. A cycle in which crystallization follows melting always exhibits hysteresis; that is, crystallization occurs at temperatures that are systematically lower than the corresponding melting temperatures. This crystallization hysteresis, illustrated in Tables I and II and in Figure 9 at 165 MPa, is due to a limited time (1.0 °C/min) allowed for crystallization. The pressure dependence of crystallization is shown in Figure 10 in the form of a series of isobaric *P–V–T* traces, in the range of 10–165 MPa. The slope dT_{crys}/dP for these data is estimated to be 0.127 °C/MPa, and the pressure versus the crystallization temperature plot is shown in Figure 11. While there is a systematic difference between the melting and crystallization temperatures, as discussed above, the slopes are essentially the same.

The kinetic effects on both melting and crystallization can be demonstrated considering the heating or cooling rate dependence, which is shown in Figure 12 for melting and Figure 13 for crystallization. At a lower heating or cooling rate, the melting point is slightly lower, while the crystallization temperature is significantly higher. As expected, in both cases, the transitions become more sharp as we decrease the rate. This means that, in principle,

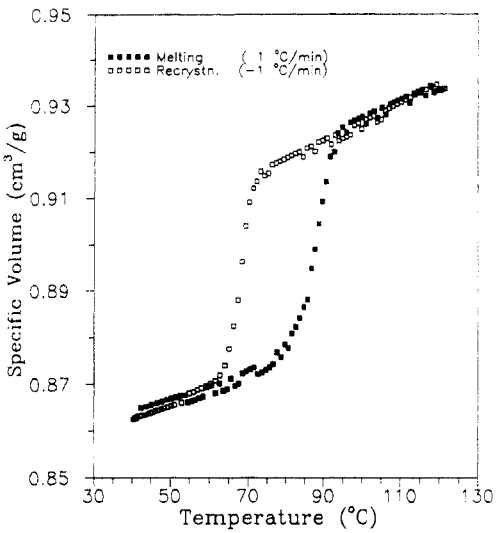

Figure 9. Comparison of PEO isobaric melting and crystallization at 165 MPa.

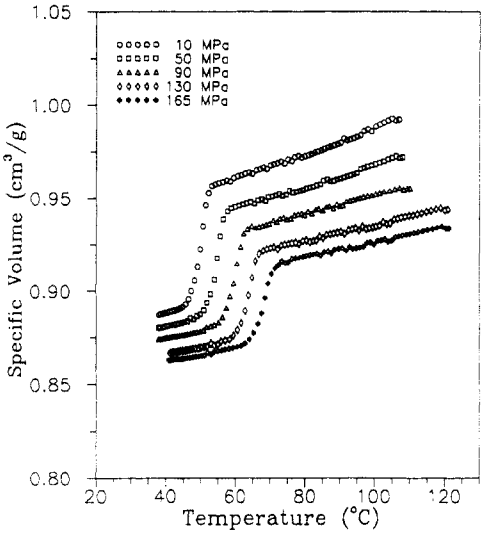

Figure 10. Isobaric crystallization of PEO at different pressures. Increasing pressures increase the crystallization temperatures.

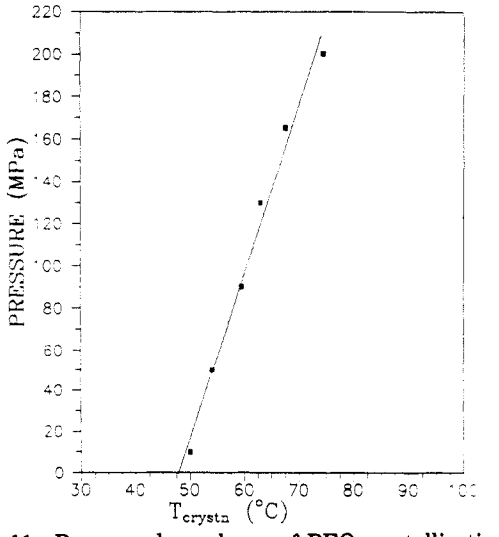

Figure 11. Pressure dependence of PEO crystallization temperature. Obtained from P–V–T measurements.

one can obtain consistent results for melting and crystallization at very low heating/cooling rates.

Estimating (dT_m/dP) from the Clapeyron Equation. The Clapeyron equation can be used to estimate the

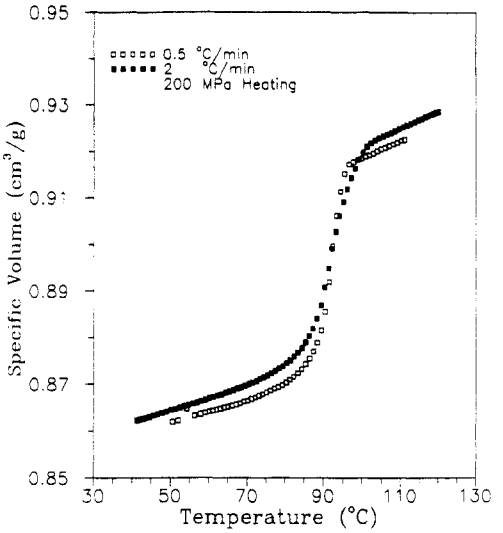

Figure 12. Effects of heating rates on PEO isobaric melting behaviors (examples at 200 MPa).

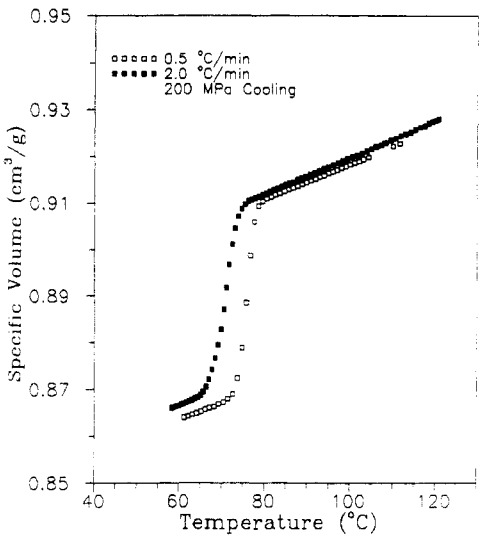

Figure 13. Effects of cooling rates on PEO isobaric crystallization behaviors (examples at 200 MPa).

pressure dependence of the melting point (dT_m/dP) from the melting expansion (ΔV_m) and enthalpy (ΔH_m), as shown in eq 1. Both ΔV_m and ΔH_m correspond to a melting transition of a fully crystalline material at T_m and P_m. However, in this work, we will use two approximations. First, we will make T_m vary linearly with pressure and, hence, make dT_m/dP constant. Second, we will use T_m, ΔV_m, and ΔH_m measured for a semicrystalline polymer at ambient pressure in the Clapeyron equation, in place of the corresponding values for a crystalline polymer at the actual P_m.

The first approximation is justified by the numerous experimental data obtained for PET,[3] PTFE,[1,4] POM,[7] nylon-6,[10] nylon-12,[11] and UDPE.[19] These data indicate that T_m varies with pressure linearly up to a few kilobars. Therefore, dT_m/dP is pressure independent and hence constant up to a few kilobars, which is our pressure range.

The second approximation is justified as follows. The Clapeyron equation has usually been used for small-molecular pure components which undergo first-order transitions, e.g., from completely crystalline to completely amorphous, or vice versa. In contrast to small molecules, real crystalline polymers are semicrystalline, i.e., only a fraction is crystalline and the balance is amorphous. Thermal expansion curves for real semicrystalline polymers should fall between the amorphous and crystalline

curves, as illustrated in ref 18. Assuming that the volume fraction of the crystalline domains is ϕ^c, we define the specific volume of a semicrystalline polymer as follows:[18]

$$V^{semi} = (1 - \phi^c)V^a + \phi^c V^c \quad (2)$$

where the superscripts a, c, and semi stand for amorphous, crystalline, and semicrystalline, respectively.

Equation 2 provides a way to interpolate between the crystalline and amorphous specific volumes using the crystalline volume fraction as the interpolation variable. At $T = T_m$ we have

$$\Delta V_m{}^c = V_m{}^a - V_m{}^c \quad (3)$$

$\Delta V_m{}^{semi}$ by definition is

$$\Delta V_m{}^{semi} = V_m{}^a - V_m{}^{semi} \quad (4)$$

Substituting eq 2 into eq 4, we obtain

$$\Delta V_m{}^{semi} = V_m{}^a - [(1 - \phi^c)V_m{}^a + \phi^c V_m{}^c]$$

and

$$\Delta V_m{}^c = \Delta V_m{}^{semi}/\phi^c \quad (5)$$

Similarly, we define the enthalpy of melting for a semicrystalline polymer as

$$\Delta H_m{}^{semi} = (1 - \phi^c)\Delta H_m{}^a + \phi^c \Delta H_m{}^c$$

Since obviously $\Delta H_m{}^a = 0$, we finally obtain a simple relationship between the crystalline and semicrystalline enthalpies:

$$\Delta H_m{}^c = \Delta H_m{}^{semi}/\phi^c \quad (6)$$

We substitute eqs 5 and 6 in eq 1:

$$\frac{dT_m}{dP} = T_m \frac{\dfrac{\Delta V_m{}^{semi}}{\phi^c}}{\dfrac{\Delta H_m{}^{semi}}{\phi^c}} = T_m \frac{\Delta V_m{}^{semi}}{\Delta H_m{}^{semi}} \quad (7)$$

We obtain an approximate Clapeyron expression that relates dT_m/dP to measurable quantities T_m, $\Delta V_m{}^{semi}$, and $\Delta H_m{}^{semi}$, all measured at ambient pressure for a semicrystalline polymer. Although in reality T_m (at constant pressure) varies slightly with crystallinity, we treat T_m as a constant with crystallinity.

In this work, we measure T_m and $\Delta H_m{}^{semi}$ on the basis of DSC. Our DSC data are reported in Table II. In summary,

$$T_m = 64.4 + 273.15 = 337.55 \text{ K}$$

$$\Delta H_m{}^{semi} = 164.8 \text{ J/g}$$

By extrapolating our P–V–T data to 0.1 MPa, we obtain

$$\Delta V_m{}^{semi} = 0.0616 \text{ cm}^3/\text{g}$$

Finally we substitute these values in eq 7 to calculate dT_m/dP:

$$\frac{dT_m}{dP} = 337.55\frac{0.0616}{164.8} = 0.126 \text{ K·cm}^3/\text{J}$$

Since $1 \text{ K·cm}^3/\text{J} = \text{K·}(10^{-6}\text{·m}^3)/(\text{kg·m}^2/\text{s}^2) = 1 \text{ K/MPa}$

$$dT_m/dP = 0.126 \text{ K/MPa}$$

This is very close to the experimental results from both high-pressure cloud-point measurements (0.111 K/MPa) and P–V–T results (0.126 K/MPa). This demonstrates that our approximation of the Clapeyron equation, using the apparent values of ΔV_m, ΔH_m, and T_m obtained for a semicrystalline PEO at ambient pressure, is quite reasonable.

Table III
Melting Point of PEO and Its Pressure Dependence from Three Different Methods

method	T°_m (°C) (at P = 0.1 MPa)	dT_m/dP (K/MPa)
cloud point	62.7	0.111
P–V–T		
heating	66.9	0.126
cooling[a]	47.9	0.127
DSC		
heating	64.4	0.126[b]
cooling[a]	47.8	0.121[b]

[a] Crystallization. [b] Calculated from the Clapeyron equation using ΔH_m and T_m from DSC and ΔV_m from P–V–T.

Similarly, the pressure dependence of the PEO crystallization temperatures can be calculated from DSC and P–V–T data (ΔH_{crys}, T_{crys}, and ΔV_{crys}, shown in Tables I and II, respectively). For PEO crystallization, the estimated value of dT_{crys}/dP is 0.121 K/MPa. The experimental result (P–V–T; Figure 11) is 0.127 K/MPa, as shown in Table III. Again, the agreement is excellent.

Another potential application of this method (Clapeyron equation coupled with ambient-pressure data) is to predict the pressure dependence for of phase transitions associated with very small values of enthalpy and volume change, e.g., polymer blends. The advantage of this approach is that ambient-pressure microcalorimeters and dilatometers are more readily available and often more accurate than high-pressure instruments.

In summary, the pressure dependence of the PEO melting derived from different methods (cloud-point, P–V–T, and DSC) is found to be consistent, in the range of 0.111–0.126 K/MPa. However, as expected, the absolute values of the melting point can vary from method to method by as much as 4 °C. This is because different methods utilize different properties associated with polymer melting.

***P–V–T* Properties of PEO Melts.** Isobaric P–V–T properties of PEO melts are characterized with the thermal expansivity which is defined as $(\partial V/\partial T)_p$. In order to quantify the thermal expansivity of PEO, we use a simple van der Waals equation of state in a form proposed by Spencer and Gilmore:[18,20,21]

$$(V - \omega)(P + \pi) = RT/M_u \quad (8)$$

where M_u is the molar mass of the "interacting unit", R is the gas constant, π is the internal pressure, and ω is the specific volume at $P = 0$ and $T = 0$. M_u, ω, and π are constants for a given polymer. Equation 8 can be rearranged as follows:

$$V = \frac{R}{M_u(P + \pi)}T + \omega \quad (9)$$

Therefore, in the plot of $V(T)$ versus T (isobaric heating or cooling), the slope is $R/[M_u(P + \pi)]$, and the intercept is ω. If the temperature is plotted in degrees Celsius ω = intercept − slope × 273.15. Figure 14 shows experimental P–V–T data and the least-square linear fits for PEO. The ω values obtained from these data vary slightly with pressure (with a maximum relative error of 3%, from 10 to 200 MPa). The value listed in Table IV is the average.

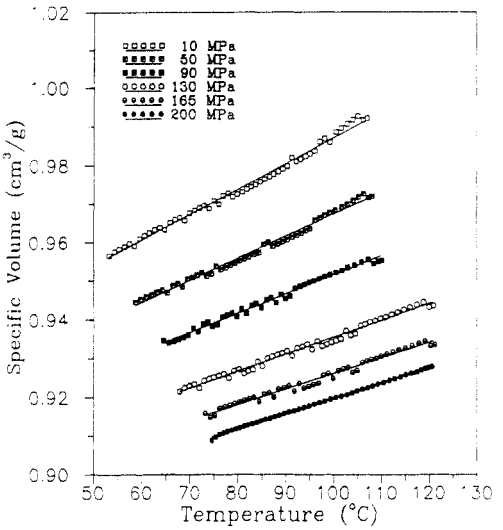

Figure 14. Isobaric expansion of PEO melts at different pressures (correlation with the Spencer–Gilmore equation).

Table IV
Equation-of-State Parameters for PEO Melts

	π (MPa)	ω (cm³/g)	M_u (g/mol)
Spencer–Gilmore			
this work	228.2	0.7638	52.77
ref 22	351	0.7355	44
	c	b_1 (MPa)	b_2 (1/°C)
Tait			
this work	0.08892	278.5	0.004918
ref 22	0.0894		
ref 25	0.0894	1335.7	0.00077 (K⁻¹)
	B_0 (MPa)	V_0 (cm³/g)	T_0 (K)
Hartmann–Haque	3334	0.8921	1623

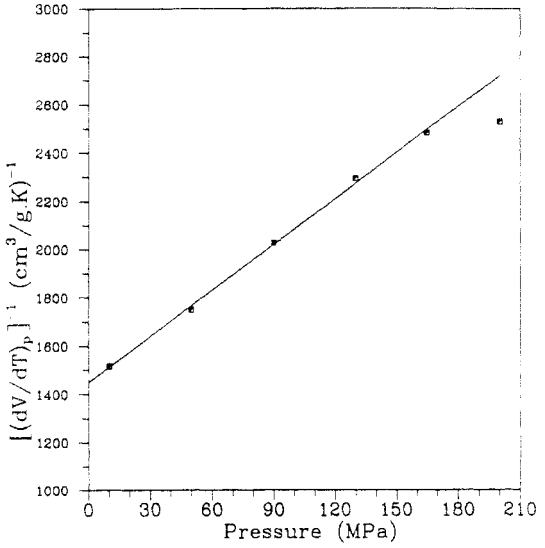

Figure 15. Variation of thermal expansivity with pressure.

The thermal expansivity $(\partial V/\partial T)_p$ can be obtained by differentiating eq 9

$$\frac{1}{(\partial V/\partial T)_p} = \left(\frac{M_u}{R}\right)P + \frac{\pi M_u}{R} \tag{10}$$

In the chart of $[(\partial V/\partial T)_p]^{-1}$ vs P, the relationship should be linear. The slope of the line is (M_u/R), and the intercept is $(\pi M_u/R)$. As shown in Figure 15, a good linear relationship has been obtained below 165 MPa for PEO. The parameters π, ω, and M_u derived from the data presented in Figure 15 are summarized in Table IV.

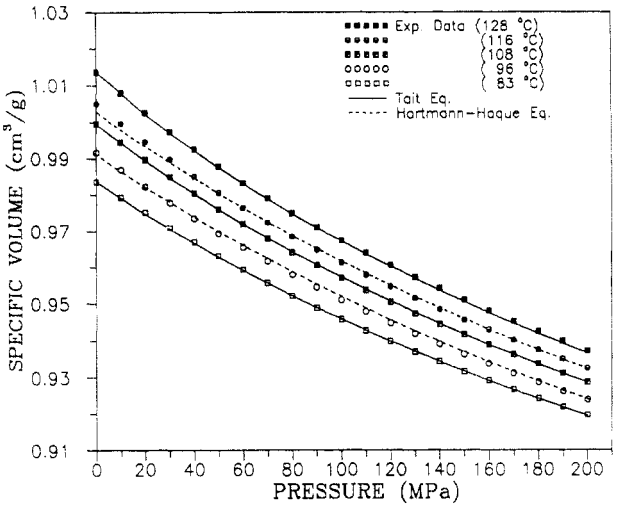

Figure 16. Isothermal compression of PEO melts at different temperatures (correlation with the Hartmann–Haque and Tait equations).

Spencer and Gilmore[18,20] suggest that M_u is equal to the molecular weight of the repeat structure unit for a linear polymer. The molar mass of $-CH_2CH_2O-$ (the structure unit of PEO) is 44.05 g/mol. Becht and co-workers[22] Use $M_u = 44$, which makes their π value much higher than ours (see Table IV). Our optimized effective value of M_u is 52.77 g/mol. Kamal and Levan[21] also suggest that M_u should be adjustable and not necessarily equal to the unit molar mass.

On the other hand, isothermal P–V–T properties of PEO melts are characterized with the compressibility which is defined as $(\partial V/\partial P)_T$. In order to quantify the compressibility of PEO we use two empirical correlations, proposed by Tait[18] and Hartmann–Haque,[18,23] respectively. The Tait equation is given by

$$\frac{V(0,T) - V(P,T)}{V(0,T)} = C \ln\left[1 + \frac{P}{B(T)}\right] \tag{11}$$

where

$$B(T) = b_1 \exp[-b_2(T - 273.15)] \tag{12}$$

The parameters C, b_1, and b_2 are constants for a given polymer.

The Hartmann–Haque equation is expressed as

$$(P/B_0)(V/V_0)^5 = (T/T_0)^{3/2} - \ln(V/V_0) \tag{13}$$

where B_0, V_0, and T_0 are constants.

Since both equations are nonlinear, we use a numerical method to fit the isothermal P–V–T data. Our fitting model is a χ^2 approach.[24] The numerical method used in solving this model is that proposed by Levenberg and Marquardt.[24] We fit the isothermal compression data at temperatures from 83 to 128 °C, in a pressure range of 0.1–200 MPa. A sample comparison of the fitting quality for both correlations is shown in Figure 16. All the parameters (C, b_1, b_2, B_0, T_0, and V_0) are summarized in Table IV.

Becht and co-workers[22] report Tait parameters for a series of PEO's with different molecular weights. However, their equation has a different format so that we can only compare the C values. Also, Jain and Simha[25] have fitted PEO P–V–T data to Tait equation-of-state parameters, as shown in Table IV. All of them use a "universal" value[18] of $C = 0.0894$, but we find that $C = 0.08892$ gives a better fit to our experimental data.

Conclusions

A new 2-kbar optical cell is developed for cloud-point measurements on polymer films. This reflect-mode cell allows for isobaric and isothermal experiments. A unique sample sandwich method prevents the pressurizing medium from contacting the polymer film.

Pressure is found to induce molecular order and, hence, shift the melting and crystallization transitions for PEO to higher temperatures. The pressure dependence is found to be linear, with a slope between 0.111 and 0.126 °C/MPa, on the basis of cloud-point, P–V–T, and DSC data.

Our Clapeyron equation approximation, using the apparent ambient-pressure values of ΔV_m^{semi} and ΔH_m^{semi} obtained for semicrystalline PEO, is demonstrated to be consistent with other methods. This approach will be of practical value where high-pressure experiments are not accurate or not possible.

Accurate P–V–T correlations for PEO melts are developed on the basis of Spencer–Gilmore, Tait, and Hartmann–Haque equations of state.

Acknowledgment. We thank D. T. Hseih for conducting the DSC experiments, C. K. Chen for help in operating the P–V–T apparatus, C. J. Gregg for assistance in designing the high-pressure optical cell, and D. J. Lohse for helpful comments that enhanced this manuscript.

References and Notes

(1) Starkweather, H. W., Jr.; Zoller, P.; Jones, G. A.; Vega, A. J. *J. Polym. Sci., Polym. Phys. Ed.* **1982**, *20*, 751.
(2) Zoller, P. *J. Polym. Sci., Polym. Phys. Ed.* **1982**, *20*, 1453.
(3) Starkweather, H. W., Jr.; Zoller, P.; Jones, G. A. *J. Polym. Sci., Polym. Phys. Ed.* **1983**, *21*, 295.
(4) Starkweather, H. W., Jr.; Zoller, P.; Jones, G. A. *J. Polym. Sci., Polym. Phys. Ed.* **1984**, *22*, 1431.
(5) Starkweather, H. W., Jr.; Zoller, P.; Jones, G. A. *J. Polym. Sci., Polym. Phys. Ed.* **1984**, *22*, 1615.
(6) Zoller, P.; Starkweather, H. W., Jr.; Jones, G. A. *J. Polym. Sci., Part B: Polym. Phys.* **1986**, *24*, 1451.
(7) Starkweather, H. W., Jr.; Jones, G. A.; Zoller, P. *J. Polym. Sci., Part B: Polym. Phys.* **1988**, *26*, 257.
(8) Zoller, P.; Kehl, T. A.; Starkweather, H. W., Jr.; Jones, G. A. *J. Polym. Sci., Part B: Polym. Phys.* **1989**, *27*, 993.
(9) Gogolewski, S.; Pennings, A. J. *Polymer* **1973**, *14*, 463.
(10) Gogolewski, S.; Pennings, A. J. *Polymer* **1975**, *16*, 673.
(11) Gogolewski, S.; Pennings, A. J. *Polymer* **1977**, *18*, 647, 654, 660.
(12) Stambuic, J. E.; Pennings, A. J. *Polymer* **1977**, *18*, 667.
(13) Hiramatsu, N.; Fukuyama, S.; Hirakawa, S. *Fukuoka Univ. Sci. Rep.* **1980**, *10*, 39, 46.
(14) Maeda, Y.; Karasz, F. E.; MacKnight, W. J. *J. Polym. Sci., Polym. Phys.* **1986**, *24*, 2345.
(15) Schouten, J. A.; Scholten, L.; Nelissen, L.; Nies, E. *Polym. Commun.* **1991**, *32*, 421.
(16) Pippard, A. B. *The Elements of Classical Thermodynamics*; Cambridge University Press: London, 1979; pp 115, 123.
(17) Zoller, P.; Bolli, P.; Pahud, V.; Ackermann, H. *Rev. Sci. Instrum.* **1976**, *47*, 948.
(18) Van Krevelen, D. W. *Properties of Polymers*, 3rd ed.; Elsevier: Amsterdam, 1990; pp 71–108 (reference for eq 2 is on p 83).
(19) Tsubakihara, S.; Nakamura, A.; Yasuniwa, M. *Polym. J.* **1991**, *23*, 1317.
(20) Spencer, R. S.; Gilmore, G. D. *J. Appl. Phys.* **1950**, *21*, 523.
(21) Kamal, H. R.; Levan, N. T. *Polym. Eng. Sci.* **1973**, *13*, 131.
(22) Becht, V. J.; Hellwege, K. H.; Knappe, W. *Kolloid Z. Z. Polym.* **1967**, *216*, 150.
(23) Hartmann, B.; Haque, M. A. *J. Appl. Polym. Sci.* **1985**, *30*, 1553.
(24) Press, W. H.; Flannery, B. P.; Teukolsky, S. A.; Vetterling, W. T. *Numerical Recipes (FORTRAN Version)*; Cambridge University Press: Cambridge, U.K., 1989; Chapter 14.
(25) Jain, R. K.; Simha, R. *J. Polym. Sci., Polym. Phys. Ed.* **1979**, *17*, 1929.